

DENSITY-BASED PARTICLE FRACTIONATION

Stefan H. Holm^{1*}, Jason P. Beech* and Jonas O. Tegenfeldt*

¹Lund University, Sweden

ABSTRACT

We present a label-free method capable of rapidly sorting particles based on their densities. Our device relies on deterministic lateral displacement (DLD) and achieves density fractionation by the use of T-shaped posts. By combining it with a lateral density gradient we achieve a density separation that is independent of size within a range given by the device geometry. Herein we present a proof-of-principle method which, in comparison to traditional density-separation techniques, is suitable for lab-on-a-chip environment.

KEYWORDS: Sorting, Separation, Density, Deterministic Lateral Displacement

INTRODUCTION

Cell density is an important biomarker which is known to vary during e.g. cell-cycle¹ and metastasizing². Further, the cell-to-cell variation in density is less than a 100-fold lower than the size variation, allowing for detection of smaller cell-perturbations³.

Commonly, density-based separations are carried out by density-gradient centrifugation⁴ which is a sensitive but also time-consuming method and on-chip integration is problematic.

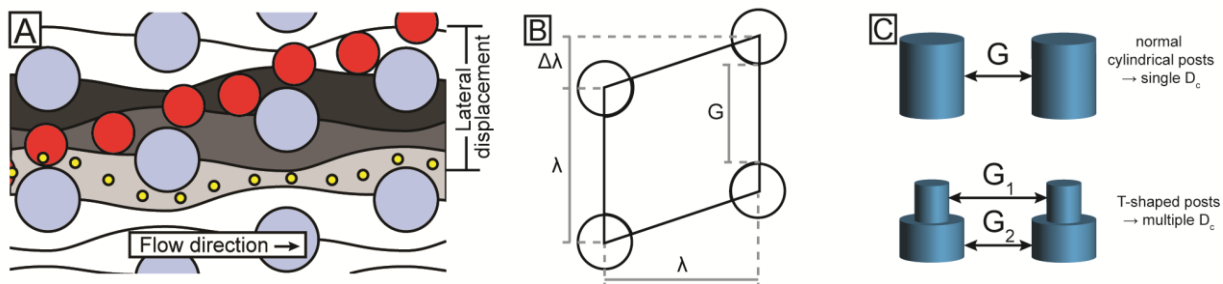
The work herein is based on DLD, a powerful and versatile particle separation technique previously shown capable of separating particles based on size⁵, shape⁶ and deformability⁷. Recently, we showed how density-based separation in DLD devices could be made possible⁸.

In DLD, particles are laterally displaced if they are larger than the critical size, which is proportional to the post-to-post distance. Thus, with T-shaped posts the particles trajectories through the device will be a function of their vertical position (Fig1A-D).

Here we extend this method by employing a density gradient across the microfluidic channel turning the bimodal separation into continuous particle fractionation.

THEORY

In DLD, an array of circular posts divides the fluid into many narrow streams Fig 1A. The widths of the stream at a given post corresponds to half the critical diameter at that particular post. Particles with a size



below this critical diameter are able to follow one such stream through the array whereas larger particles

Figure 1: (A) Schematic illustration showing a section of a DLD device, with posts coloured blue. The hydrodynamic centre of the small yellow particle is able to fit within the gray flow stream while the larger red particle is laterally displaced to the adjacent flow stream for each row. (B) A unit cell in the DLD array showing the gap and the center-to-center distance between to neighboring posts, λ . (C) Illustration showing the normal cylindrical posts and the T-shaped posts used in this work. With T-shaped posts two different gaps, and consequently two separate critical diameters are present. As a result, the particles vertical position determines their trajectory through the device..

are forced, through hydrodynamic and steric interactions with the posts, to change streams in each subsequent row leading to a lateral displacement. For spherical particles the critical diameter, D_c , at which this transition between following the flow (zigzagging mode) and being displaced (displacement mode) occurs is given by eqn (1)

$$D_c = 1.4GN^{-0.48} \quad (1)$$

with the parameters given in Fig 1B. Thus, the critical diameter is a function of the periodicity of the array, N , and more important for this work the distance between two posts, the gap (G).

Traditionally, the posts of a DLD device have been cylindrical, which then produces a single specific gap and consequently a single critical size. However, by the use of T-shaped posts, Fig 1C, we obtain a device with two distinct gaps and consequently two separate critical sizes. The device was designed with an upper gap which resulted in a D_c larger than all particle sizes and a small lower gap resulting in a D_c smaller than all particle sizes, Fig 1C. Consequently, any particle which resides in the lower section will be laterally displaced while if they float up into the large gap section they will stop being laterally displaced.

EXPERIMENTAL

A master for replica molding was fabricated using two precisely aligned UV-lithography (MJB4, SUSS-MicroTec, Germany) steps in 8 μm thick SU8 (MicroChem, USA) on silicon wafers. Devices were then produced using standard soft lithography and bonded to a glass slide with oxygen plasma (Plasmatic Systems Inc, USA). Pressure was used to induce flow (MFCS-FLEX, Fluigent, France).

The sample consisted of three different types of microspheres of similar sizes but different materials and consequently densities; i) polystyrene (1.05 g/cm³ 4.87 \pm 0.28 μm , Polysciences Inc, USA). ii) melamin (1.57g/cm³ 4.74 \pm 0.14 μm , Sigma-Aldrich, USA). iii) silicon (2.33 g/cm³, 4.63 \pm 0.46 μm , Bangs laboratories, USA) in a buffer of density $\rho_1 = 1.22$ g/cm³ while the density of the clean buffer was $\rho_2 = 1.98$ g/cm³. The buffer densities were set by the addition of sodium-polytungstate (Na-PTS, #71913, Sigma-Aldrich).

A MATLAB script (MathWorks, USA) was used to determine the lateral position of each particle at the outlet. The critical diameter of the device is 3 μm for the lower gap and 7 μm for the large top gap, below and above the particle size.

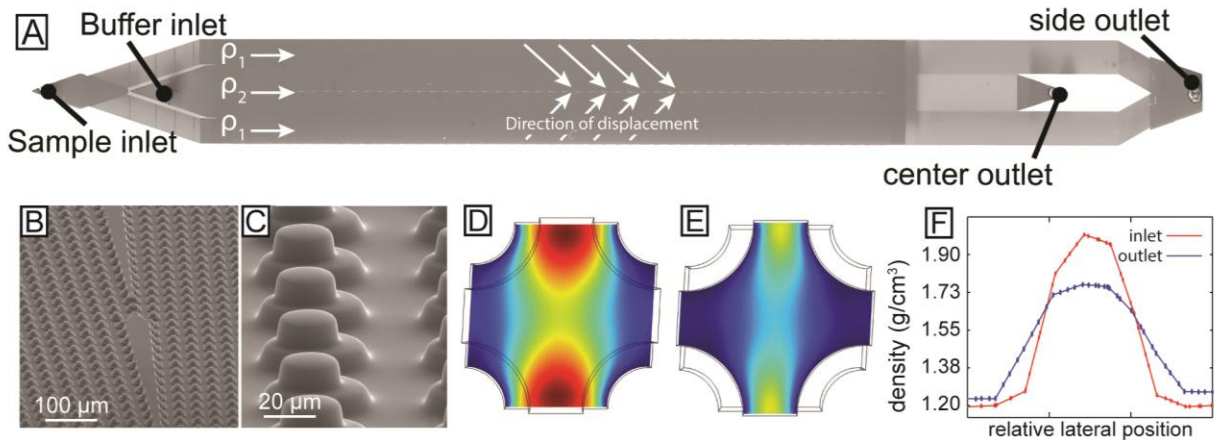


Figure 2: (A) micrograph of our device showing the mirrored design with a buffer inlet and a sample inlet which is split up into two. The densities of the fluids are, $\rho_1 = 1.22$ g/cm³ and $\rho_2 = 1.98$ g/cm³. (B-C) higher magnification micrographs showing the T-shaped posts. (D-E) FEM simulations of a unit cell in the device confirming the critical size being consistent with eqn (1). (F) FEM simulations showing the density distribution at the inlet and the outlet at a flow speed of 1 mm/s.

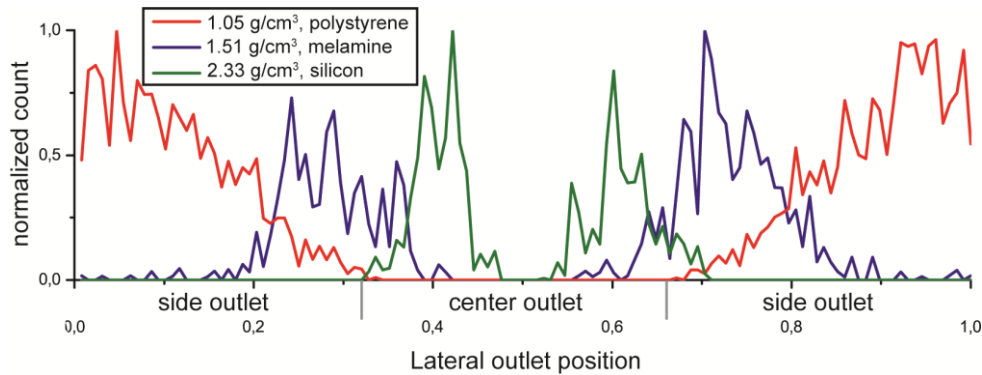


Figure 3: Particle distribution at the end of the device. Due to the buoyancy of the lighter particles they float up to the large gap section and consequently they zigzag through the device, ending up in the side outlet. The high density silicon particles, sediment into the small gap and are laterally displaced in the whole device, ending up in the center outlet. The melamin particles have a higher density than the first buffer but lower density than the second buffer (ρ_1 and ρ_2 in Fig 2A). This makes these particles become laterally displaced in the beginning but after a distance they are laterally displaced into the second buffer making them float up into the large gap section, making them zigzag in the overall flow direction.

RESULTS AND DISCUSSION

The particle distribution at the outlet is given in Figure 3. The melamine and silicon particles have a higher density (1.51 and 2.33 g/cm³ respectively) than the buffer they are suspended in from the beginning (1.22 g/cm³). Consequently, in the device they sediment to the lower level with smaller gaps. As the particles are larger (~4.7 μ m) than this critical diameter (3 μ m) they are displaced towards the center outlet. Eventually they are displaced into the higher density buffer (1.98 g/cm³) where the melamine particles float up to the level with larger gap and stop being displaced while the silicon particles continue to be displaced toward the center. The polystyrene particles, on the other hand, have a lower density (1.05 g/cm³) than both buffers making them float up into the large gap, with a large critical diameter, they are not displaced and end up in the side outlets at the end of the device.

CONCLUSION

We have successfully demonstrated a proof-of-principle for a microfluidic device sensitive to particle density. The device can easily be integrated in a lab-on-chip environment as it is based on the passive and continuous separation technique DLD. Focus for future experiment include evaluate the sensitivity for enabling cell-measurements and to increase throughput.

ACKNOWLEDGEMENTS

The work presented herein was made possible by the support of the Nanometer Structure Consortium at Lund University (nmC@LU).

REFERENCES

1. L. H. Hartwell, *Journal of Bacteriology*, 1970, 104, 1280-1285.
2. K. Bosslet, R. Ruffmann, P. Altevogt and V. Schirmacher, *Br J Cancer*, 1981, 44, 356-362.
3. W. H. Grover, A. K. Bryan, M. Diez-Silva, S. Suresh, J. M. Higgins and S. R. Manalis, *PNAS*, 2012, 109, 1523-1529.
4. T. Timonen and E. Saksela, *Journal of Immunological Methods*, 1980, 36, 285-291.
5. L. R. Huang, E. C. Cox, R. H. Austin and J. C. Sturm, *Science*, 2004, 304, 987-990.
6. S. H. Holm, J. P. Beech, M. P. Barrett and J. O. Tegenfeldt, *Lab on a Chip*, 2011, 11, 1326-1332.
7. J. P. Beech, S. H. Holm, K. Adolfsson and J. O. Tegenfeldt, *Lab on a Chip*, 2012, 12, 1048-1051.
8. S. H. Holm, J. P. Beech and J. O. Tegenfeldt, presented in part at the MicroTAS 2013, the 17th International Conference on Miniaturized Systems for Chemistry and Life Sciences, Freiburg, Germany, 2013.

CONTACT

* S.H. Holm, tel: +46 (0)70-4099380; Stefan.Holm@ftf.lth.se